On the atomic structure of liquid Ni–Si alloys: a neutron diffraction study

2009 J. Phys.: Condens. Matter 21 385403

(http://iopscience.iop.org/0953-8984/21/38/385403)

J. Phys.: Condens. Matter **21** (2009) 385403 (7pp) doi:10.1088/0953-8984/21/38/385403

On the atomic structure of liquid Ni–Si alloys: a neutron diffraction study

S Gruner[1,5], J Marczinke[1], L Hennet[2], W Hoyer[1] and G J Cuello[3,4]

[1] Institute of Physics, Chemnitz University of Technology, D-09107 Chemnitz, Germany
[2] CNRS-CEMHTI, University of Orléans, F-45071 Orléans, France
[3] Institute Laue-Langevin, PO Box 156, F-38042 Grenoble, France
[4] Basque Country University, PO Box 644, E-48080 Bilbao, Spain

E-mail: sascha.gruner@physik.tu-chemnitz.de

Received 11 May 2009, in final form 8 July 2009
Published 24 August 2009
Online at stacks.iop.org/JPhysCM/21/385403

Abstract
The atomic structure of the liquid NiSi and $NiSi_2$ alloys is investigated by means of neutron diffraction experiments with isotopic substitution. From experimental data-sets obtained using four Ni isotopes, partial structure factors and pair correlation functions are obtained by applying a reverse Monte Carlo modelling approach. Both alloys were found to exhibit a strong tendency to hetero-coordination within the first coordination shell. In particular, covalent Si–Si bonds with somewhat greater distances seem to influence the structure of the liquid NiSi alloy.

1. Introduction

Nickel based alloys cover a wide field of application, such as light-weight cast alloys with high mechanical strength at elevated temperatures. Suitable alloys are obtained by adding aluminium or silicon. Thus, great effort has been made to investigate the physical properties of these materials, both in the solid as well as the liquid state. Obviously, the latter is especially important for further optimization of production processes.

From a physical point of view the question arises to what extent the atomic structure of the liquid material is governed by the tendency to covalent interactions introduced by Si. An analysis given by Kita *et al* [1] demonstrated that a certain degree of covalency is expected in Si-rich transition metal (TM)–silicon alloys, resulting in a distinct second Si–Si distance of about 3.7 Å. On the other hand, molten compound-forming alloys are often described in terms of associates embedded in a matrix of the remaining atoms. The stoichiometry and atomic arrangement within these clusters is believed to resemble that of the most stable intermetallic phases present in the solid state. This approach is quite successful interpreting the isothermal composition dependences of thermophysical properties such as the dynamic viscosity, which often show pronounced maxima at the composition of intermetallic compounds.

[5] Author to whom any correspondence should be addressed.

In this work we present a neutron diffraction study on the liquid NiSi and $NiSi_2$ alloys. In order to obtain structural information on all the possible atom pairs Ni–Ni, Ni–Si as well as Si–Si separately, the neutron diffraction experiments were carried out in conjunction with isotopic substitution.

Both compositions chosen for this study form intermetallic compounds in the solid state. The $NiSi_2$ crystallizes in an ordered CaF_2-type super-structure [2], with unlike atoms approaching closest to each other ($r_{NiSi} = 2.33$ Å). Each of the Ni atoms is surrounded by $N_{NiSi} = 8$ Si atoms and, vice versa, $N_{SiNi} = 4$. The distances between nearest like atoms are $r_{SiSi} = 2.69$ Å and $r_{NiNi} = 3.81$ Å, respectively. The $NiSi_2$ compound decomposes into Si and liquid alloy at a temperature of 993 °C. The NiSi crystal, on the other hand, has less symmetry: the unit cell is orthorhombic and the atoms form hetero-coordinated layers linked by Ni–Ni neighbours [2]. The NiSi-compound has a melting temperature of about 990 °C.

2. Experimental details

2.1. Neutron diffraction

The neutron diffraction experiments reported here have been carried out at the dedicated liquid and amorphous substances diffractometer D4c at the Institute Laue-Langevin, Grenoble, France. The instrument set-up is described in detail in [3]. The wavelength of the incident neutrons was calibrated by means of a crystalline Ni reference sample and found to be $\lambda = 0.6975$ Å. Thus, the range of the modulus of the

diffraction vector covered by these experiments is 0.25 $\text{Å}^{-1} \leqslant Q \leqslant 16.8\ \text{Å}^{-1}$.

For the present study, an aerodynamic levitation technique has been applied. By means of a remote-controlled jet of purified argon a small spherical sample (diameter of about 2.5 mm) is lifted from a nozzle of suitable geometry in such a way that the specimen has no contact to any material and about two thirds of the sample are illuminated by the neutron beam. The sample was heated from top to the desired temperature, which has been pyrometrically monitored, by means of two CO_2 lasers. Further details of the levitator and its mounting to D4's sample position are given in [4]. Special care has been taken placing a B_4C shielding in order to avoid background scattering from the nozzle itself.

Details of the data refinement are given in [5]. The treatment included the usual corrections for the background contribution as well as multiple and inelastic scattering and normalization with respect to a Vanadium reference sample of the same geometry. The obtained differential scattering cross section is converted into Faber–Ziman total structure factors $S^{\text{FZ}}(Q)$ [6] by using the relation

$$\langle b\rangle^2 S^{\text{FZ}}(Q) = \frac{\mathrm{d}\sigma}{\mathrm{d}\Omega} - (\langle b^2\rangle - \langle b\rangle^2), \tag{1}$$

with the angle brackets denoting the composition average over the coherent scattering lengths b of the constituents.

Due to the small sample volume, the total structure factors recorded in reasonable counting time are rather noisy. However, it was demonstrated by Hoyer *et al* [7] that $S^{\text{FZ}}(Q)$ can be expressed as

$$S^{\text{FZ}}(Q) = S^{\text{FZ}}(Q=0) + \alpha Q^2 \tag{2a}$$

for small values of Q and

$$S^{\text{FZ}}(Q) = 1 + A\cos(BQ - C)\frac{\exp(-DQ)}{Q} \tag{2b}$$

in the high-Q region. The parameters α, A, B and D are to be determined by least-square fitting procedures to the experimental data. Finally, the structure factors have been extrapolated for $Q \to 0$ using (2*a*) and substituted by (2*b*) for $Q > 6\ \text{Å}^{-1}$, the choice of which has been tested not to influence the further analysis. This procedure has two major advantages: (i) the noise is reduced without simultaneously smoothing out the meaningful oscillations and (ii) as both relations (2*a*) and (2*b*) can be Fourier transformed analytically, total pair correlation functions calculated by

$$g^{\text{FZ}}(r) = 1 + \frac{1}{2\pi^2\rho_0}\int_0^\infty \mathrm{d}Q\,Q^2\frac{\sin(Qr)}{Qr}[S^{\text{FZ}}(Q) - 1] \tag{3}$$

do not show any spurious features due to truncation effects.

In accordance with earlier experiences we estimate the experimental error in the height of the total structure factors as well as pair correlation functions does not exceed 5%. This is especially true as the corrections due to parasitic scattering is small with the set-up used. The applied fitting procedure is helpful in detecting minor distortions due to improper corrections, which have not been observed here. The peak positions in both Q- and r-space correlation functions are expected to be accurate to better than 2%.

Table 1. Weighting factors w_{ij} with which the partial structure factors contribute to the experimental total structure factors obtained with the different Ni isotopes used.

Ni isotope used	NiSi			$NiSi_2$		
	w_{NiNi}	$2w_{\text{NiSi}}$	w_{SiSi}	w_{NiNi}	$2w_{\text{NiSi}}$	w_{SiSi}
*Ni	0.508	0.409	0.083	0.307	0.494	0.199
^{58}Ni	0.603	0.347	0.050	0.402	0.464	0.134
^{60}Ni	0.162	0.481	0.357	0.064	0.377	0.559
^{62}Ni	3.658	−3.490	0.832	477.828	−911.939	435.111

2.2. Samples

Ingots of the alloys NiSi and $NiSi_2$ have been prepared from the pure constituents by means of arc-melting in high purity inert gas (Ar), split into pieces of the proper volume and again arc-melted to an approximate spherical shape which is necessary for successfully starting the levitation process. During this procedure, neither a loss of sample mass due to evaporation nor oxidation of the sample's surface has been observed. Pure silicon (purity 99.999%, $b = 4.15$ fm) and four different isotopic mixtures of Ni have been used: (i) the natural isotopic mixture *Ni ($b = 10.31$ fm) (ii); ^{58}Ni (enrichment: 99.8%, $b = 14.4$ fm); (iii) ^{60}Ni (enrichment: 99.6%, $b = 2.8$ fm) and (iv) ^{62}Ni (enrichment: 97.9%, $b = -8.7$ fm).

In order to obtain a maximum of information on the short- and medium-range order we chose a temperature close above (about 50 K) the liquidus line of the two alloys studied.

3. Results

3.1. Total structure factors

The obtained total Faber–Ziman structure factors for both alloys under investigation are shown in figure 1 and the total pair correlation functions $g^{\text{FZ}}(r)$ calculated by equation (3) are given in figure 2. Please note the change in the scale for the ^{62}Ni-measurements, for which the right ordinates apply. The large differences in the magnitudes impressively illustrate that the total interference functions contain averaged structural information weighted with the scattering power and the concentration of the involved atomic species:

$$S^{\text{FZ}}(Q) = \sum_i\sum_j \frac{c_i c_j b_i b_j}{\langle b\rangle^2} S_{ij}(Q) = \sum_i\sum_j w_{ij} S_{ij}(Q). \tag{4a}$$

The $S_{ij}(Q)$ denote the so-called partial structure factors which describe the contribution of atomic pairs i–j to the total scattered intensity. The weighting factors w_{ij} for the alloys and isotopic mixtures studied here are listed in table 1. The use of the ^{62}Ni isotope with its negative scattering length results in the unusual weighting factors for these samples as well as the enhanced amplitudes in the total structure factors. Anyway, the value $\langle b\rangle$ for the alloy containing ^{62}Ni is still well above zero, thus the w_{ij} are well defined and the Faber–Ziman formalism may be applied.

For neutron diffraction experiments, where the neutron scattering lengths b_i do not depend on the absolute value of the

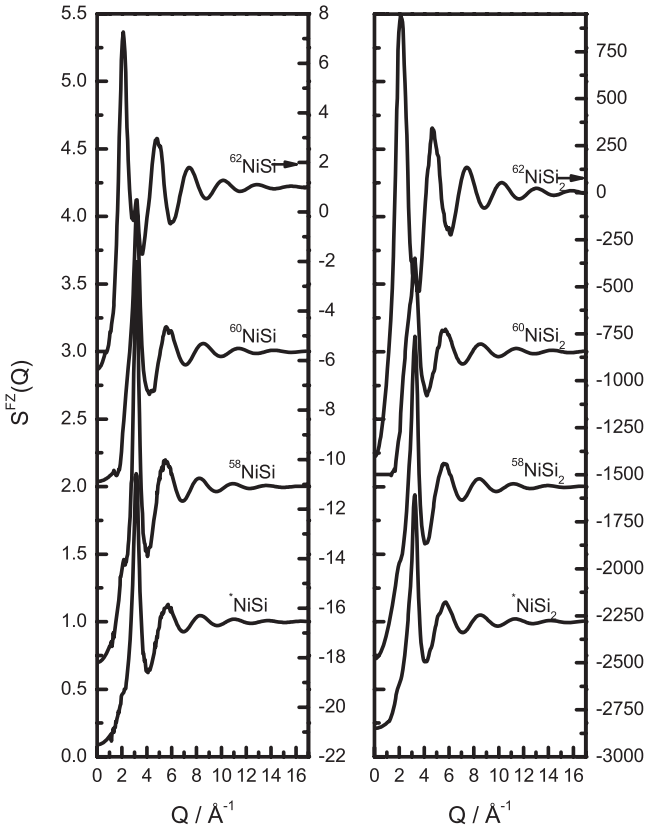

Figure 1. Total Faber–Ziman structure factors of the liquid NiSi (left) and $NiSi_2$ (right) alloy. Please note that the right ordinates apply for the ^{62}Ni-measurement, only. For clarity, the curves are shifted by one, subsequently.

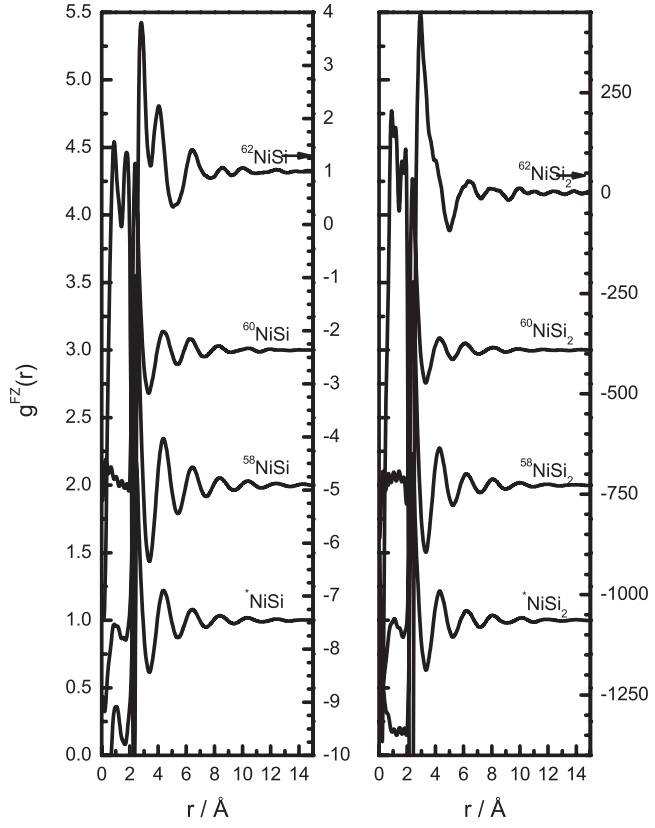

Figure 2. Total pair correlation functions of the liquid NiSi (left) and $NiSi_2$ (right) alloy obtained by Fourier transformation of the $S^{FZ}(Q)$. Please note that the right ordinates apply for the ^{62}Ni-measurement, only. For clarity, the curves are shifted by one, subsequently.

diffraction vector Q, the same relation can be used to introduce the partial pair correlation functions $g_{ij}(r)$:

$$g^{FZ}(r) = \sum_i \sum_j \frac{c_i c_j b_i b_j}{\langle b \rangle^2} g_{ij}(r). \qquad (4b)$$

The $g_{ij}(r)$, describing the probability of finding an atom of species j at a distance r from a central atom of species i, contains the most detailed structural information to be obtained from diffraction experiments. The Fourier transformation, as given by equation (3), relates the $S_{ij}(Q)$ to the $g_{ij}(r)$.

However, bearing the nature of the differences in the $S^{FZ}(Q)$ in mind, certain statements can already be made from comparisons of the total structure factors and pair correlation functions, especially as the Ni–Si pairs contribute with negative weighting to the ^{62}Ni-data: (i) like atoms contribute to the total structure factors at small Q (around 2 Å^{-1}), while the Ni–Si pair contributes at about 3.2 Å^{-1}; (ii) the pre-peak in the total structure factors, most pronounced in the ^{58}Ni-data at about 2 Å^{-1}, should be attributed to Ni–Ni pairs; (iii) in real-space, unlike atoms approach closer than like atoms, clearly seen in a negative contribution in the ^{62}Ni–$g^{FZ}(r)$; (iv) ordering, visible by oscillations in the $g^{FZ}(r)$, occurs up to distances of about 14 Å; (v) as these oscillations in the ^{62}Ni-data are shifted against those in the other $g^{FZ}(r)$, the ordering seems to be of chemical rather than just topological nature.

3.2. Partial structure factors and partial pair correlation functions

Following equation (4*a*) a set of three equations containing three experimental total structure factors is to be solved in order to obtain the three partial structure factors $S_{NiNi}(Q)$, $S_{NiSi}(Q) = S_{SiNi}(Q)$ and $S_{SiSi}(Q)$. The available experimental data-sets (in the following we shall denote them just by the kind of Ni isotope used) can thus be combined to four systems of equations which, according to the different weighting of the $S_{ij}(Q)$, contain different amounts and kinds of information. The normalized determinant ($\det \boldsymbol{C}$) of the coefficient-matrix can be used as a measure of this [8]. A digest on the possible sets of equations and the resulting determinants is given in table 2. It is noteworthy that the combination's determinants differ by nearly a factor of ten. Thus one might expect rather different resulting partial structure factors, the more reliable ones being obtained from the (*Ni, ^{60}Ni, ^{62}Ni) as well as (^{58}Ni, ^{60}Ni, ^{62}Ni) combinations.

The calculated partial structure factors are depicted in figure 3. As expected, remarkable differences occur in the curves, rendering some curves physically senseless. However, the curves obtained from the combinations mentioned above do agree very well and only those should be considered further.

In order to make use of all four available data-sets simultaneously, the reverse Monte Carlo modelling technique (RMC)—see [9, 10] for details—has been applied. Basically,

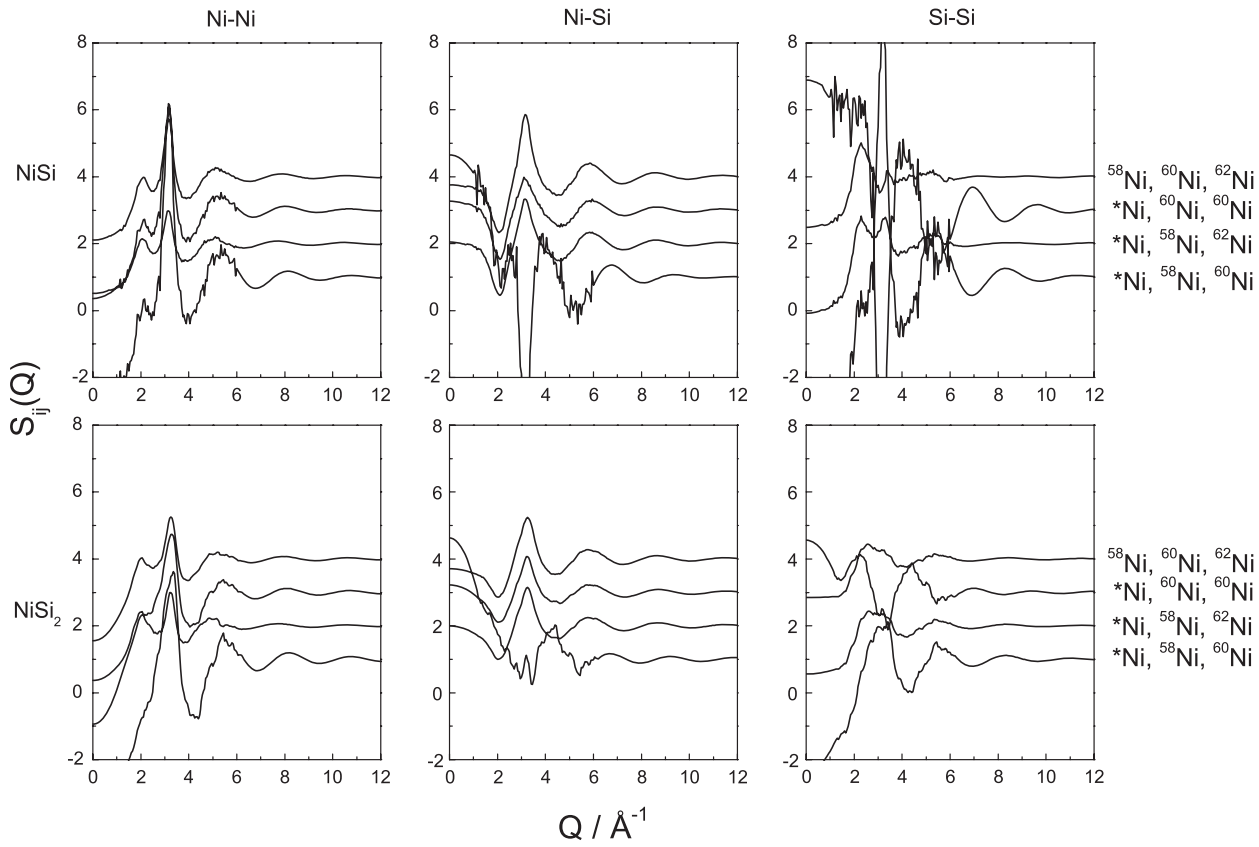

Figure 3. Calculated partial structure factors for the NiSi (top) and $NiSi_2$ (bottom) alloy. The lines represent the different systems of equations used. For clarity of the presentation the Q-range has been limited to 12 $Å^{-1}$.

Table 2. Four systems of equations can be set up to calculate the three partial structure factors from four experiments. The determinants can be used as a measure of the structural information incorporated.

Used data-sets (Ni isotopes)	(det C_{NiSi})	(det C_{NiSi_2})
*Ni, ^{58}Ni, ^{60}Ni	0.036	0.042
*Ni, ^{60}Ni, ^{62}Ni	0.391	0.438
*Ni, ^{58}Ni, ^{62}Ni	0.064	0.135
^{58}Ni, ^{60}Ni, ^{62}Ni	0.435	0.567

the deviations between the model's total structure factors and the experimental ones is to be minimized by random moves of atoms within a cubic simulation box with periodic boundary conditions. During the modelling process the proper number density ρ_0 is to be respected. For the present modelling, an initial random configuration of 3000 atoms has been chosen and ρ_0 has been calculated from the densities of the pure constituents assuming a constant molar volume. Further details on the modelling process as well as a discussion on the reliability of the models obtained is to be found in [11].

From the model configuration the partial pair correlation functions and, by Fourier transformation, the partial structure factors can be calculated. The results are compared to the $S_{ij}(Q)$ obtained by direct solution of equation (4*a*) in figure 4 and the agreement is found to be remarkably good. This finding encourages the use of the model obtained from the RMC procedure for the further analysis. In doing so, the information of all four total structure factors is used and, furthermore, a three-dimensional atomic configuration can be investigated. The structural model obtained is necessarily built up from spheres placed in a sensible manner, i.e. no overlap occurs. Therefore, the RMC algorithm itself implies a constraint on the $g_{ij}(r)$: they are necessarily non-negative in the whole r-range and equal to zero for small values of r. Thus, application of the RMC algorithm avoids the percolation of uncertainties due to normalization and truncation in the resulting partial pair correlation functions.

The partial structure factors of the liquid NiSi and $NiSi_2$ are rather similar. As already discussed above, the Ni–Ni partial structure factor exhibits a pronounced pre-maximum for both alloys. At the same Q-position a deep minimum is observed in $S_{NiSi}(Q)$. The Ni–Ni and Ni–Si partial structure factors are rather similar in their further behaviour, especially the positions of the first maxima are equal and oscillations occur in the whole Q-range covered by the experiments. However, the Si–Si contribution shows a broad maximum for the $NiSi_2$ alloy, which splits into two components for the NiSi composition. Visible oscillations range further in the case of the $NiSi_2$ alloy, and the overall shape of $S_{SiSi}(Q)$ resembles that of the structure factor of pure molten silicon [12] for that alloy. It should be pointed out that neither the pre-peak in $S_{NiNi}(Q)$ nor the minimum in $S_{NiSi}(Q)$ has been found in the anomalous x-ray scattering study reported by Waseda and Tamaki [13].

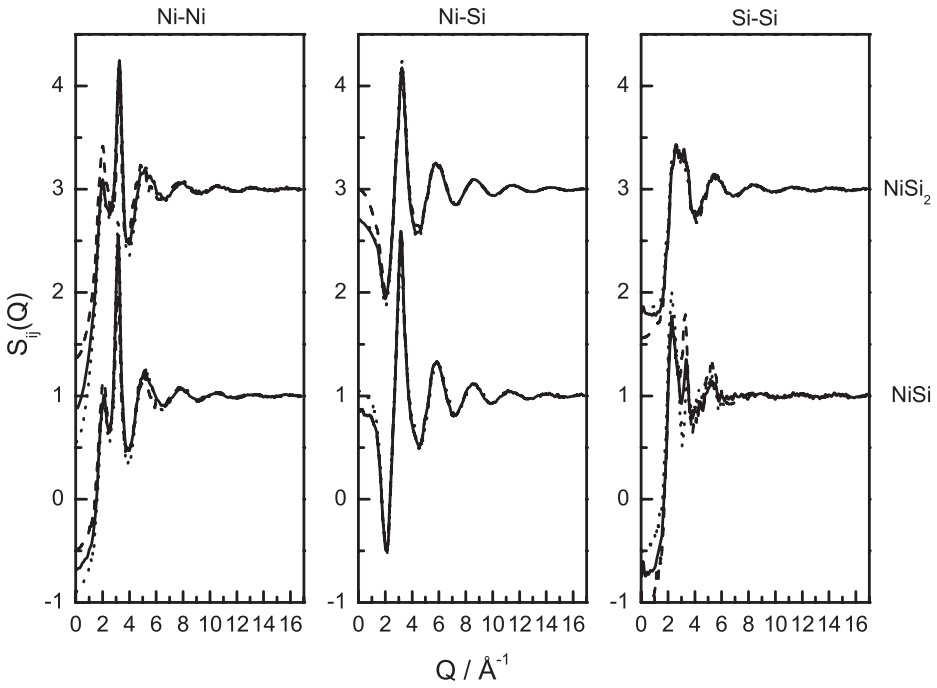

Figure 4. Comparison of the partial structure factors obtained by solution of equation (4) (dash—*Ni, ^{58}Ni, ^{62}Ni, dot—^{58}Ni, ^{60}Ni, ^{62}Ni) and RMC modelling (solid—all data-sets). The curves for the $NiSi_2$ alloy have been shifted for clarity.

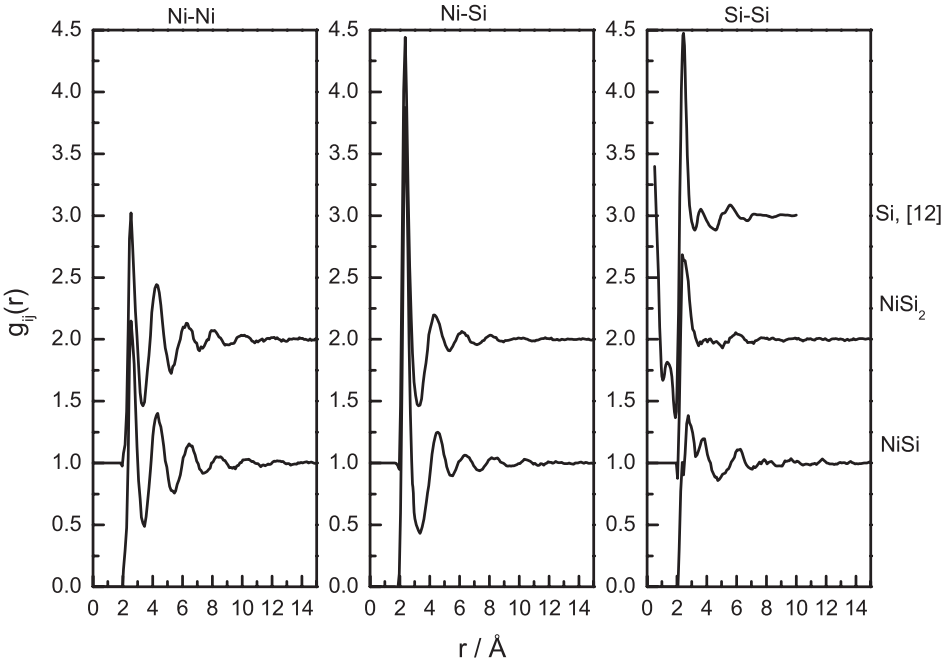

Figure 5. Partial pair correlation functions of the NiSi (bottom) and $NiSi_2$ (top) liquid alloys obtained from the RMC model. For comparison, the pair correlation function of pure liquid silicon is added. The curves have been shifted by one, subsequently.

Figure 5 shows the partial pair correlation functions obtained directly from the model configuration for both alloys under investigation. By integrating $\rho_j g_{ij}(r) = c_j \rho_0 g_{ij}(r)$ in spherical coordinates in the range of the first coordination shell (i.e. up to the first minimum in the respective $r^2 g_{ij}(r)$) one yields the partial coordination numbers:

$$N_{ij}^{\mathrm{I}} = 4\pi c_j \rho_0 \int_0^{r_{\min}} \mathrm{d}r\, r^2 g_{ij}(r). \tag{5}$$

The radii of the coordination shells as well as the partial coordination numbers are listed in table 3. Most remarkably, unlike atoms approach each other closer than the like atoms in both alloys. The Ni–Si first coordination shell is rather sharp compared to those of the other pairs. The correlation between the distances between Ni atoms long up to 14–15 Å, while the correlations for the other pairs are rather limited. The first Si–Si shell is splitted into two sub-shells in the case of the NiSi alloys.

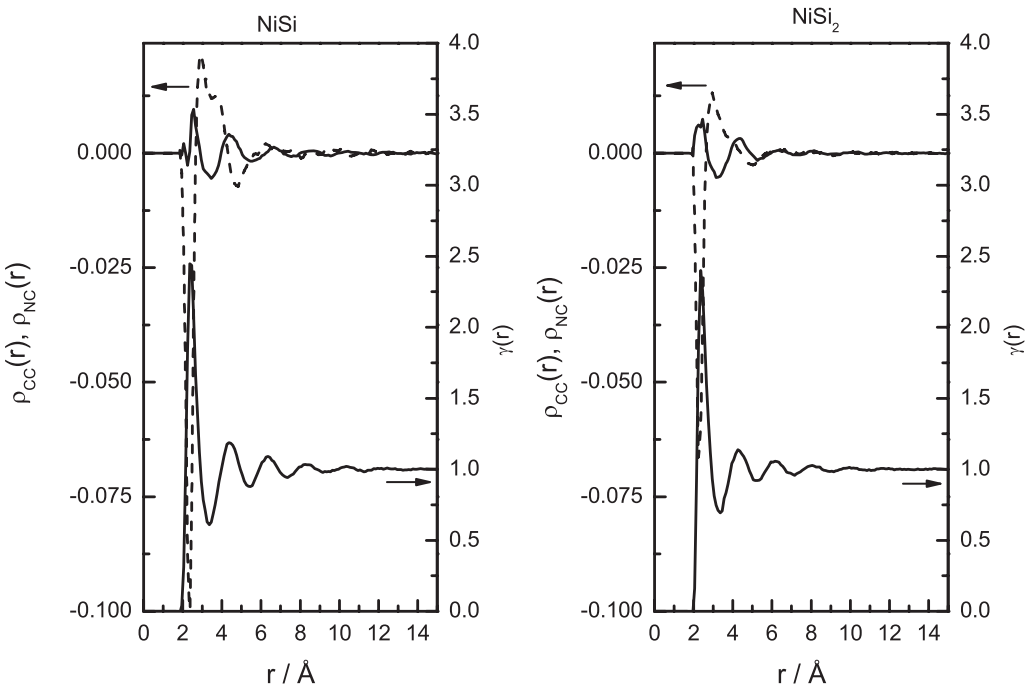

Figure 6. Concentration correlation function (dashed line), density–concentration correlation function (upper solid line) and absolute total pair correlation functions (lower solid line) obtained from equation (7). The common interpretation of these curves allows to analyse the occupation of the individual coordination shells.

Table 3. Main structural parameters: radii of the coordination spheres, partial coordination numbers and short-range order parameter.

	NiSi				$NiSi_2$			
	Ni–Ni	Ni–Si	Si–Ni	Si–Si	Ni–Ni	Ni–Si	Si–Ni	Si–Si
r^{I} (Å)	2.59	2.37		2.77 (3.72)	2.54	2.35		2.53
r^{II} (Å)	4.35	4.54		6.16	4.28	4.38		6.03
$r^{\mathrm{II}}/r^{\mathrm{I}}$	1.68	1.92		2.22	1.69	1.86		2.38
N^{I}	4.9	5.4	5.4	4.2	2.5	6.5	3.2	4.7
$N^{\mathrm{I}}_{\mathrm{Ni}}$		10.3				9.0		
$N^{\mathrm{I}}_{\mathrm{Si}}$		9.6				7.9		
$\langle N^{\mathrm{I}}\rangle$		10.0				8.3		
η		0.09				0.14		

Taking into account that all uncertainties resulting from the experiment, the corrections and the calculation of the $g_{ij}(r)$ accumulate in the partial coordination numbers we estimate them to be accurate to the order of 10%. However, the radii of the coordination shells are well defined due to the high scattering contrast implied by the ^{62}Ni measurement and we account an uncertainty of about 2% as well.

4. Discussion

The coordination numbers and pair separations listed in table 3 clearly evidence a deviation from both the hard-sphere behaviour discussed in [13] and the random distribution of the atoms in both studied liquid alloys. The short-range order parameter

$$\eta = \frac{N^{\mathrm{I}}_{\mathrm{NiSi}}\langle N^{\mathrm{I}}\rangle}{c_{\mathrm{Si}}N^{\mathrm{I}}_{\mathrm{Ni}}N^{\mathrm{I}}_{\mathrm{Si}}} - 1 \tag{6}$$

introduced by Cargill and Spaepen [14], with $N^{\mathrm{I}}_i = N^{\mathrm{I}}_{ii} + N^{\mathrm{I}}_{ij}$ and $\langle N^{\mathrm{I}}\rangle = c_{\mathrm{Ni}}N^{\mathrm{I}}_{\mathrm{Ni}} + c_{\mathrm{Si}}N^{\mathrm{I}}_{\mathrm{Si}}$, takes positive values pointing towards a preference of pairs of unlike atoms in the first coordination shell. This obviously agrees well with the unlike atoms approaching closer to each other. The average coordination number is slightly larger in the NiSi alloy than in the $NiSi_2$ alloy.

In order to elucidate this further, one can calculate the radial concentration correlation function

$$\rho_{\mathrm{CC}}(r) = \rho_0 c_{\mathrm{Si}}c_{\mathrm{Ni}}[g_{\mathrm{NiNi}}(r) + g_{\mathrm{SiSi}}(r) - 2g_{\mathrm{NiSi}}(r)] \tag{7a}$$

as introduced by Ruppersberg and Egger [15] and

$$\rho_{\mathrm{NC}} = \rho_0 c_{\mathrm{Si}}c_{\mathrm{Ni}}[c_{\mathrm{Ni}}g_{\mathrm{NiNi}}(r) + c_{\mathrm{Si}}g_{\mathrm{NiSi}}(r) - c_{\mathrm{Ni}}g_{\mathrm{NiSi}}(r) - c_{\mathrm{Si}}g_{\mathrm{SiSi}}(r)]. \tag{7b}$$

The former relation directly indicates preferred distances of like atoms by taking positive values while hetero-coordinated coordination spheres are marked by a negative ρ_{CC}. The latter function compares the local number densities around central atoms of the individual species. Both functions are depicted in figure 6 together with an absolute total pair correlation function

$$\gamma(r) = \sum_i \sum_j c_i c_j g_{ij}(r) \tag{7c}$$

indicating the coordination spheres. In fact, these three functions are related to the Bhatia–Thornton partial structure

factors [16] by Fourier transformations. The occupation of the coordination shells now becomes obvious: as already stated, the first coordination shell is dominated by unlike atoms (negative ρ_{CC}) and a rather dense packing of atoms around Ni. In the following, less occupied shell, the like atoms are preferred. ρ_{CC} shows a splitting, indicating that two distances occur. The right-hand side part thereof at $r = 3.7$ Å coincides with the minimum in ρ_{NC} and is therefore supposed to describe the surrounding of silicon atoms. Si–Si correlations at such a distance have been interpreted as signs of covalency by Kita *et al* [1]. On the base of a peak decomposition they found a certain degree of covalent bonding to be present in the liquid Si-TM alloys at higher Si-contents. However, from our recent analysis it seems that a portion of the silicon atoms forms covalent bonds even in the NiSi alloy. In the partial Si–Si pair correlation function this manifests in the right-hand sub-peak for the NiSi alloy and a less pronounced hump for the $NiSi_2$.

The further coordination shells are marked by an increased packing density around Ni atoms. Remarkably, in the $NiSi_2$ alloy $\gamma(r)$, $\rho_{CC}(r)$ and $\rho_{NC}(r)$ have their maxima and minima in the same positions, indicating a preference of like atoms. In the NiSi alloy, the coordination spheres seem to be split up into sub-shells of like (smaller distances) and unlike (larger distances) atoms.

From the calculated three-dimensional configuration of atoms one can deduct the bond-angle distribution functions. In the case of Ni-centred triplets, the obtained curves are rather broad, allowing bond angles between 60° and 120° with nearly equal probability. On the other hand, Si-centred triplets occur most frequently with an internal angle of about 110°, pointing to tetrahedral configurations of neighbours around Si, matching the decreased local density found for Si–Si distances. Once again, this is more pronounced in NiSi.

In summary, one can state that the NiSi alloy's structure seems to be strongly influenced by Si's tendency to form covalent bonds. The indications of covalent behaviour are less pronounced in the $NiSi_2$ alloy and it seems that the liquid's structure is still influenced by the ordered salt-like structure adopted in the solid state. For instance, the short-range order parameter takes a higher value and the partial Ni–Si and Si–Ni coordination numbers are only slightly reduced in favour of pairs of like atoms, a behaviour which is clearly due to the thermal disorder in the melt.

Finally, the pre-peak in the Ni–Ni partial structure factor and coincidentally a minimum in $S_{NiSi}(Q)$ is, following a discussion by Enderby [17], a result of a charge transfer between the species and was similarly found in the liquid eutectic $NiGe_2$ alloy [18].

The presented findings contradict the results given by Waseda and Tamaki [13], who found the partial correlation functions to be independent of the concentration and, moreover, a hard spheres description to be suitable. Clearly, a chemical short-range ordering occurs in both investigated alloys.

5. Conclusions

The atomic structure of liquid NiSi and $NiSi_2$ has been studied by means of neutron diffraction with isotopic substitution. It was demonstrated that for the determination of reliable partial structure factors, combination of data-sets with sufficient information is required. The information of all available total structure factors has been incorporated within models derived by means of the reverse Monte Carlo technique.

Both alloys exhibit a strong tendency to hetero-coordination in the first coordination shell and a certain charge transfer between the species is observed. The local number density is reduced around silicon atoms. In conjunction with preferred bond angles of about 110° in Si-centred triplets and a characteristic atomic separation of 3.7 Å this evidences covalent bonds formed by a certain degree of Si atoms. It seems that the atomic structure of the liquid NiSi alloy is strongly influenced by Si's tendency to forming covalent bonds, while the structure of liquid $NiSi_2$ moreover resembles that of the ordered solid alloy.

Acknowledgments

Three of us (SG, JM and LH) gratefully acknowledge financial support by the Institute Laue-Langevin under proposal no. 6-03-375. We wish to thank the whole D4c-team for their help and support during the experiments. The research has been founded by the Deutsche Forschungsgemeinschaft (DFG) under the grant-no. HO1688/14-1.

References

[1] Kita Y, Van Zytveld J B, Morita Z and Iida T 1994 *J. Phys.: Condens. Matter* **6** 811–20
[2] Villars P and Calvert L D (ed) 1996 *Pearson's Handbook of Crystallographic Data for Intermetallic Phases* (Metals Park, OH: American Society for Metals)
[3] Fischer H E, Cuello G J, Palleau P, Feltin D, Barnes A C and Simonson J M 2002 *Appl. Phys.* A **74** S160–2
[4] Hennet L *et al* 2006 *Rev. Sci. Instrum.* **77** 053903
[5] Cuello G J 2008 *J. Phys.: Condens. Matter* **20** 244109
[6] Faber T E and Ziman J M 1965 *Phil. Mag.* **11** 153–173
[7] Hoyer W, Kaban I and Halm Th 2001 *J. Optoelectron. Adv. Mater.* **3** 255–64
[8] Edwards F G, Enderby J E, Howe R A and Page D I 1975 *J. Phys. C: Solid State Phys.* **8** 3483–90
[9] McGreevy R L and Pusztai L 1988 *Mol. Simul.* **1** 359–67
[10] McGreevy R L 2001 *J. Phys.: Condens. Matter* **13** R877–913
[11] Gruner S, Akinlade O and Hoyer W 2006 *J. Phys.: Condens. Matter* **18** 4773–80
[12] Waseda Y 1980 *The Structure of Non-Crystalline Materials* (New York: McGraw-Hill)
[13] Waseda Y and Tamaki S 1975 *Phil. Mag.* **32** 951–60
[14] Cargill G S and Spaepen F 1981 *J. Non-Cryst. Solids* **43** 91–7
[15] Ruppersberg H and Egger H 1975 *J. Chem. Phys.* **63** 4095–103
[16] Bhatia A B and Thornton D E 1970 *Phys. Rev.* B **2** 3004–12
[17] Enderby J E 1982 *J. Phys. C: Solid State Phys.* **15** 4609–25
[18] Halm Th, Hoyer W, Neumann H and Bellisent R 1993 *Z. Naturforsch.* a **48** 452–6